

Single-Crystal X-Ray Diffraction and Electronic Band Structure Studies of PdTeI

D.-K. Seo and M.-H. Whangbo¹

Department of Chemistry, North Carolina State University, Raleigh, North Carolina 27695-8204

and

K. Neininger and G. Thiele¹

Institut für Anorganische Chemie, Albertstrasse 21, D-79104 Freiburg, Germany

Received July 25, 1997; accepted October 22, 1997

The crystal structure of PdTeI was determined by single-crystal X-ray diffraction measurements, and its electronic band structure was calculated using the extended-Hückel tight-binding method. Each Pd³⁺ (*d*⁷) cation of PdTeI is located at a distorted octahedral site, so that PdTeI has four half-filled *z*² bands dispersive mainly along the *c* direction. Thus, optical and transport properties of PdTeI are predicted to be highly one-dimensional, although the crystal structure of PdTeI is three-dimensional. Implications of the crystal and electronic structures on the physical properties of PdTeI are discussed. © 1998 Academic Press

1. INTRODUCTION

The synthesis and crystal structure of palladium telluride iodide, PdTeI, were briefly reported nearly two decades ago (1). This compound has an unusual oxidation state Pd³⁺ (*d*⁷) and has a three-dimensional (3D) extended structure. In addition, its color is brass yellow, so PdTeI is expected to be either a metal or a semiconductor with a small band gap. So far, details of the crystal structure of PdTeI have not been reported in the literature. Since the common oxidation states of Pd are +2 and +4, one may wonder if PdTeI is susceptible to a distortion leading to a mixed-valence state (2, 3). In the present work, we describe the crystal structure of PdTeI determined from single-crystal X-ray diffraction measurements (4) and examine its electronic structure by performing extended-Hückel tight-binding (EHTB) electronic band structure calculations (5).

¹To whom correspondence should be addressed.

2. EXPERIMENTAL

Single crystals of PdTeI were prepared by reaction of 50 mg of Pd (about 0.47 mmol), 60 mg of Te (about 0.47 mmol), and 120 mg I₂ (about 0.47 mmol) in about 2 ml of HI (56%) with about 30 mg of KI (about 0.18 mmol) in a sealed silica ampoule (0.8-mm diameter, 4-cm length) at 300°C for 2 weeks. The method has been previously described (1, 6).

X-ray diffraction measurements were carried out using a single crystal (size: 0.025 × 0.03 × 0.25 mm³) on a four-circle diffractometer (Enraf-Nonius CAD-4). The structure was determined using direct methods of SHELXS86 (7) and refined with SHELXL93 (8). The absorption correction was carried out using the empirical program XABS2 (9). A summary of data collection and refinement data is given in Table 1. The fractional atomic coordinates and anisotropic displacement parameters are summarized in Table 2, and some geometrical parameters are listed in Table 3.

3. CRYSTAL STRUCTURE

It is convenient to describe the crystal structure of PdTeI in terms of the planar Te₂PdI₂ unit **1**, in which Te...Te = 3.385 Å and I...I = 3.809 Å (Table 3). The ladder chain **2** is obtained from Te₂PdI₂ units by sharing their Te...Te and I...I edges such that the Te...Te and I...I edges alternate along the chain direction. The Pd...Pd distance bridged by the Te atoms is slightly longer than that bridged by the I atoms (3.952 versus 3.873 Å). To construct the 3D lattice of PdTeI, we form the layer **3a** of equally spaced ladder chains running along the *a* direction using the *a* axis length as the spacing between them, form the layer **3b** in a similar manner using the ladder chains running along the *b* axis, and stack the layers **3a** and **3b** by alternating

TABLE 1
Crystal Data and Information about Data Collection
and Structure Refinement

(A) Crystal data	
PdTeI	MoK α radiation
$M_r = 360.90$	$\lambda = 0.71073 \text{ \AA}$
Tetragonal	$\mu = 22.245 \text{ mm}^{-1}$
$P4_2/mmc$	Needle
$a = 7.821(1) \text{ \AA}$	$0.025 \times 0.03 \times 0.25 \text{ mm}^3$
$c = 5.659(1) \text{ \AA}$	Brass yellow
$V = 346.15(9) \text{ \AA}^3$	$T = 298 \text{ K}$
$Z = 4$	25 reflections measured
	$\theta = 5\text{--}25^\circ$
(B) Data collection	
Enraf-Nonius CAD-4 diffractometer	$\theta = 3.65\text{--}34.94^\circ$
$\omega\text{--}2\theta$	$-12 \leq h \leq 8;$
	$-12 \leq k \leq 12; 0 \leq l \leq 9$
Absorption correction: XABS (9)	2914 reflections
463 independent reflections	
401 observed reflections [$I > 2\sigma(I)$]	
(C) Structure determination and refinement	
SHELXS86 (7)	SHELXL93 (8)
$R(F)$ (obs refl) = 1.54%	$\Delta\rho_{\min} = -0.95 \text{ e/\AA}^3$
$wR(F^2)$ (all refl) = 3.63%	$\Delta\rho_{\max} = 2.19 \text{ e/\AA}^3$
GOOF (all refl) = 1.095	$0.946 \leq t \leq 1.129$
13 parameters	

them along the c direction such that the Te atoms form squares in a projection view of the 3D lattice along the c direction (see 4). Consequently, each Pd $^{3+}$ cation forms a distorted PdTe $_4$ I $_2$ octahedron (see 5), and PdTeI has the formula (PdTeI) $_4$ per unit cell. It is important to distinguish the Pd–Te bond within a ladder chain (i.e., Pd–Te $_{\parallel}$) from that between adjacent ladder chains (i.e., Pd–Te $_{\perp}$). The Pd–Te $_{\perp}$ bonds are not perpendicular to the plane of the ribbon chain but are tilted toward the adjacent Te \cdots Te edge of the ribbon chain so that Te $_{\perp}$ –Pd–Te $_{\perp} = 168.62(2)^\circ$ (Table 3).

4. ELECTRONIC STRUCTURE

Given the local coordinate system shown in 5, the t_{2g} levels of a regular octahedral PdL $_6$ are described by the

TABLE 2
Fractional Atomic Coordinates (in 10^4) and Anisotropic
Displacement Parameters (in 10^3 \AA^2)

Atom	x	y	z	U_{11}	U_{22}	U_{33}
Pd	0	2525(1)	0	14(1)	14(1)	13(1)
Te	2164(1)	0	0	14(1)	14(1)	16(1)
I	2435(1)	5000	0	15(1)	13(1)	37(1)

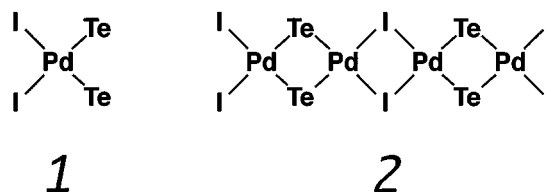
TABLE 3
Some Geometrical Parameters of PdTeI

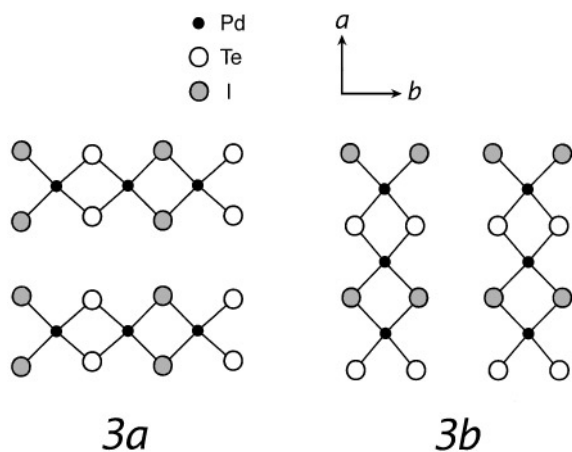
Bond lengths (\AA)	Bond angles (deg)
Pd–Te $_{\parallel} = 2.601(1)$	Te $_{\parallel}$ –Pd–Te $_{\parallel} = 81.2(1)$
Pd–Te $_{\perp} = 2.844(1)$	I–Pd–I = 89.06(1)
Pd–I = 2.715(1)	Te $_{\perp}$ –Pd–Te $_{\perp} = 168.62(2)$
Pd \cdots Pd = 3.873(1), 3.952(1)	
Te $_{\parallel}\cdots$ Te $_{\parallel} = 3.385(1)$	
Te $_{\parallel}\cdots$ Te $_{\perp} = 3.706(1)$	
I \cdots I = 3.809(1)	

xz , yz , and $x^2 - y^2$ orbitals of Pd, and the e_g levels by the xy and z^2 orbitals of Pd. In the distorted octahedron PdTe $_4$ I $_2$ of each Pd $^{3+}$ (d^7) cation, the Pd–Te $_{\perp}$ bond is longer than the Pd–Te $_{\parallel}$ bond, and the Pd–Te $_{\perp}$ bonds are tilted away from the z axis. Thus, the e_g levels are split as depicted in 6, so that the z^2 level is lower than the xy level and is singly filled. The z^2 orbital of each Pd $^{3+}$ can overlap effectively only with the Te p_z orbitals of the Pd–Te $_{\perp}$ bonds. Each –Pd–Te $_{\perp}$ –Pd–Te $_{\perp}$ – chain along the c direction leads to a z^2 band, so PdTeI will have four z^2 bands because it has four Pd $^{3+}$ ions per unit cell. These bands will be dispersive mainly along the c direction and half-filled as a whole.

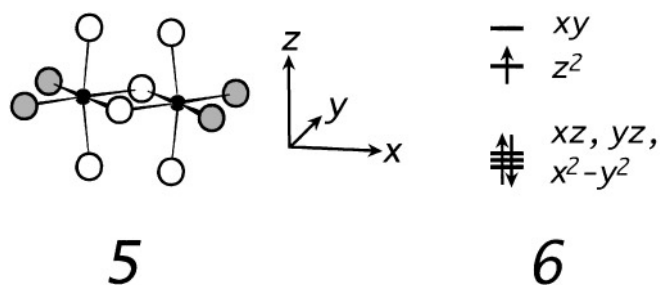
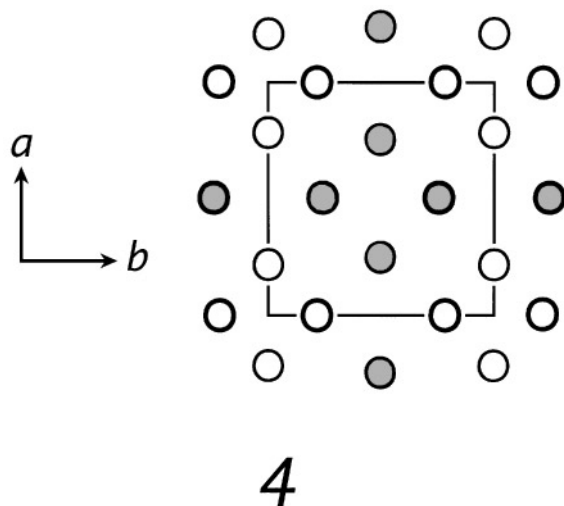
The foregoing expectations are confirmed in the present EHTB electronic band structure calculations for PdTeI. The atomic parameters employed in our calculations are summarized in Table 4. Figure 1a presents dispersion relations of the d -block bands (near the Fermi level) calculated for PdTeI. Four bands dispersive only the c direction are cut by the Fermi level (the middle of the three bands crossing the Fermi level is doubly degenerate). The projected density of states calculated for the z^2 and xy orbitals of Pd is shown in Fig. 1b, and those for the $x^2 - y^2$ and xz orbitals of Pd are shown in Fig. 1c. It is clear from Fig. 1b that the dispersive bands crossing the Fermi level are based on the z^2 orbitals of Pd. The width of the z^2 bands is about 2 eV.

Figures 1a–c suggest that PdTeI is a one-dimensional (1D) metal with four half-filled bands and is therefore susceptible to a charge density instability (10–12) that opens a band gap at the Fermi level and leads to a doubling of the c -axis length. Such a distortion can be modeled by introducing small displacements δ of the Pd, Te, or I atoms. Two examples of the Te atom displacements leading to





a c -axis doubling are presented in **7a** and **7b**. The displacements are along the c direction in **7a** and along the ladder chain directions in **7b**. In a similar manner, a c -axis doubling can be achieved by displacing the I atoms along the c direction (**7c**). Figure 2a shows the dispersion relations of the bands calculated for PdTeI with a unit cell doubled along the c direction but without any atom displacement. The dispersion relations along Γ -Z are identical to those of Fig. 1a, except for the folding of the bands that occurs due to the unit cell doubling. When the Te atom displacement of $\delta = 0.05 \text{ \AA}$ is introduced according to the dimerization model **7a**, the z^2 bands are split as shown in Fig. 2b, thereby producing a band gap of $\sim 0.2 \text{ eV}$. For the dimerization model **7b**, the Te atom displacement is not effective in opening a band gap; Fig. 2c shows that the split z^2 bands still overlap for $\delta = 0.10 \text{ \AA}$. The dimerization model **7c** is even less effective in opening a band gap, because Fig. 2d shows that the split bands strongly overlap even for $\delta = 0.10 \text{ \AA}$. This is due to the fact that the I atom contributions to the z^2 bands are not strong. Thus, a displacement of



Te (equivalently, that of Pd) along the c direction most effectively introduces a band gap. The distortions **7a** and **7b** generate two different Pd sites, but **7c** does not. In the z^2 band and Pd z^2 orbitals have antibonding interactions with the Te p_z orbitals in each $-\text{Pd}-\text{Te}_\perp-\text{Pd}-\text{Te}_\perp-$ chain along the c direction. Therefore the dimerization mode **7a** is most effective in producing two different Pd sites and hence introducing a band gap.

5. CONCLUDING REMARKS

According to the crystal structure of PdTeI, each Pd^{3+} (d^7) ion is located in a distorted PdTe_4I_2 octahedron such that z^2 level of PdTe_4I_2 is singly filled. Consequently, PdTeI has four half-filled z^2 bands, which are dispersive mainly along the c direction. It is expected that the polarized reflectivity of PdTeI is high when the electric vector of the light is parallel to the c direction and vanishes when the electric vector is perpendicular to the c direction. The electrical property of PdTeI should be highly anisotropic with least resistivity along the c direction. Preliminary electrical resistivity measurements based on a pressed pellet of PdTeI samples suggest a semiconducting behavior around room

TABLE 4

Exponent ζ_i and Valence Shell Ionization Potentials H_{ii} of Slater-Type Orbitals χ_i Used for Extended-Hückel Tight-Binding Calculation^a

Atom	χ_i	H_{ii} (eV)	ζ_i	c_1^b	ζ'_i	c_2^b
Pd	5s	-7.32	2.19	1.0		
Pd	5p	-3.75	2.15	1.0		
Pd	4d	-12.0	5.983	0.5264	2.613	0.6373
Te	5s	-20.8	2.51	1.0		
Te	5p	-13.2	2.16	1.0		
I	5s	-18.0	2.679	1.0		
I	5p	-12.7	2.322	1.0		

^a H_{ii} 's are the diagonal matrix elements $\langle \chi_i | H^{\text{eff}} | \chi_i \rangle$, where H^{eff} is the effective Hamiltonian. In our calculations of the off-diagonal matrix elements $H^{\text{eff}} = \langle \chi_i | H^{\text{eff}} | \chi_j \rangle$, the weighted formula was used. See J. Ammeter, H.-B. Bürgi, J. Thibeault, and R. Hoffmann, *J. Am. Chem. Soc.* **100**, 3686 (1978).

^b Contraction coefficients used in the double- (ζ) , Slater-type orbital.

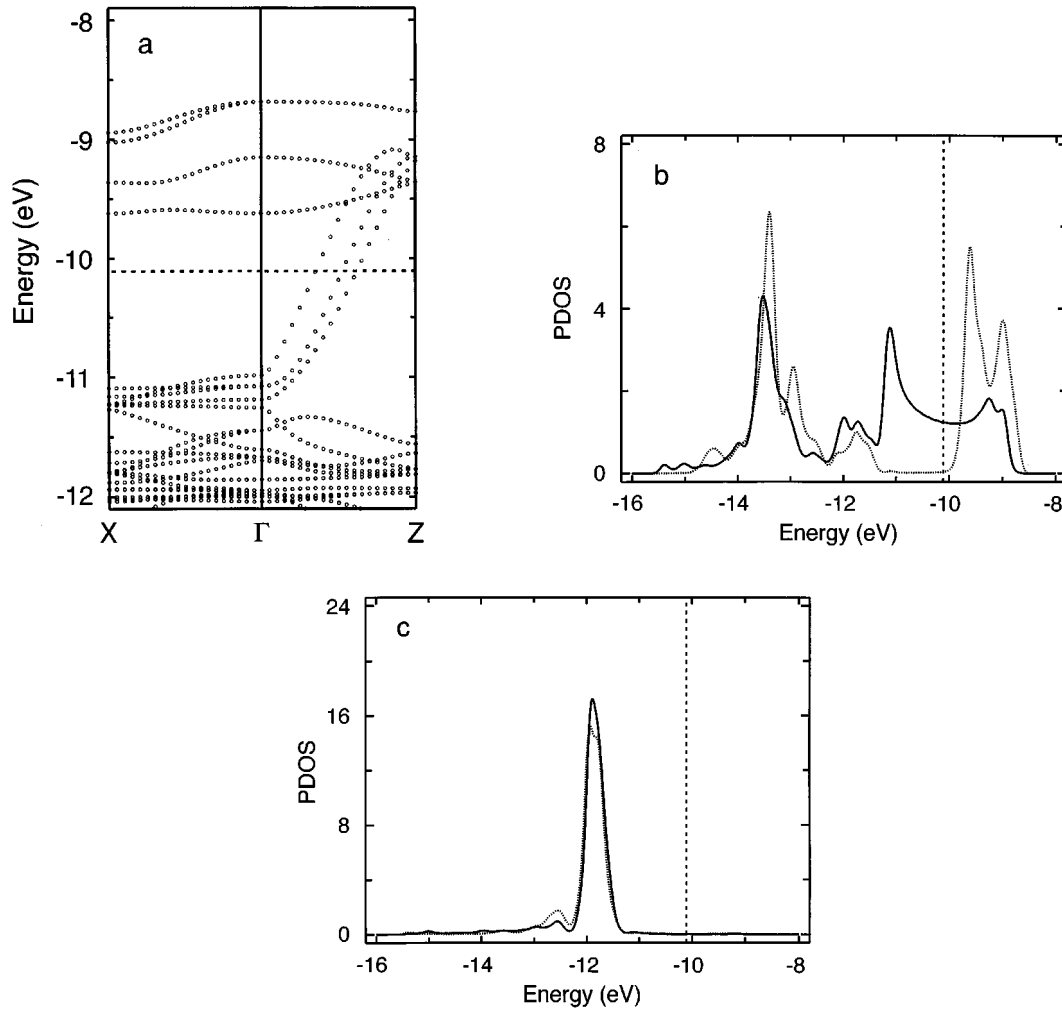


FIG. 1. Calculated electronic structure of PdTeI. (a) Dispersion relations of the top portion of the d -block bands calculated for PdTeI. The dashed line is the Fermi level, $\Gamma = (0, 0, 0)$, $X = (a^*/2, 0, 0)$, and $Z = (0, 0, c^*/2)$. (b) Projected density of state (PDOS) plots calculated for the z^2 (solid line) and xy (dotted line) orbitals of Pd, where the dashed line is the Fermi level. (c) PDOS plots calculated for the $x^2 - y^2$ (solid line) and xz (dotted line) of Pd. The PDOS plot for the yz orbital is identical with that for the xz orbital.

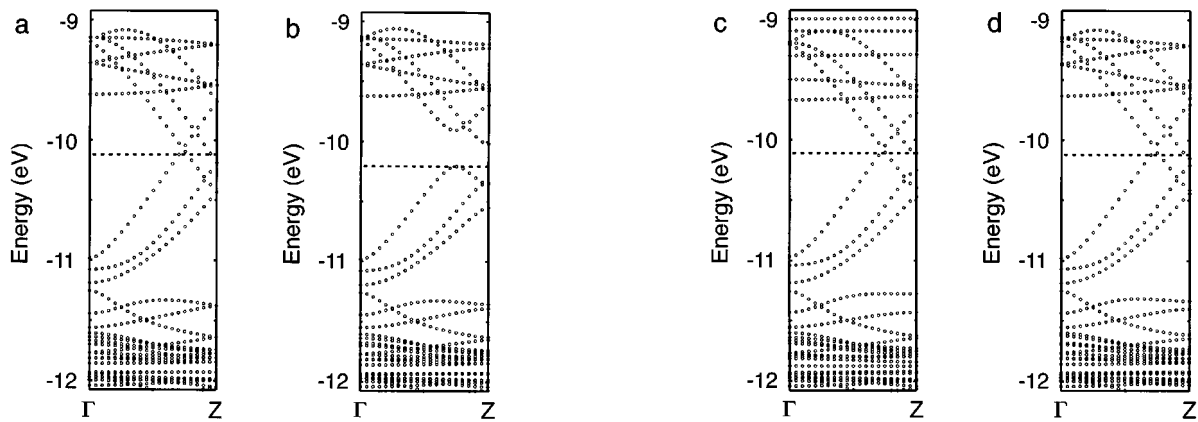
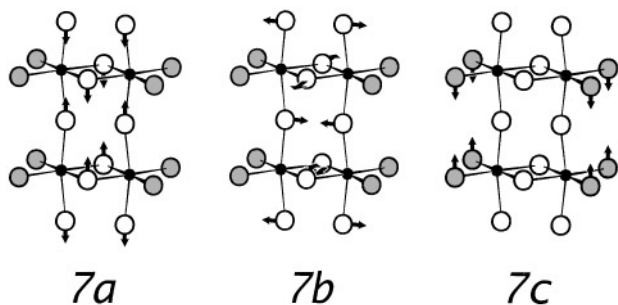


FIG. 2. Dispersion relations of the top portion of the d -block bands calculated for PdTeI along Γ - Z : (a) for a unit cell doubled along the c direction but without any atom displacement, (b) for a dimerization model **7a** with $\delta = 0.05 \text{ \AA}$, (c) for a dimerization model **7b** with $\delta = 0.10 \text{ \AA}$, and (d) for a dimerization model **7c** with $\delta = 0.10 \text{ \AA}$.



temperature (4). Thus, by analogy with the crystal structure and semiconducting property of $(\text{Et}_4\text{N})_4[\text{AuAg}_2\text{Sn}_2\text{Te}_9]$ (13), it is tempting to speculate that PdTeI has already undergone a c -axis-doubling distortion at room temperature. However, the anisotropic displacement parameters of Table 2 do not exhibit any substantial elongation along the c axis for Pd and Te. The anisotropic parameters of I have an elongation along the c axis, but our discussion in the previous section showed that any pairing distortion involving the I atom is not effective in introducing a band gap. Accurate resistivity measurements using single-crystal samples of PdTeI are necessary to determine if PdTeI is a metal, a semiconductor, or a magnetic semiconductor. In addition, it is desirable to determine the crystal structure of PdTeI at a low temperature to see if a c -axis-doubling distortion takes place upon lowering the temperature.

ACKNOWLEDGMENTS

This work was supported by the U.S. Department of Energy, Office of Basic Sciences, Division of Materials Sciences, under Grant DE-FG05-86ER45259 and also by the Alexander von Humboldt Foundation.

REFERENCES

1. G. Thiele, M. Köhler-Degner, K. Wittmann, and G. Zoubek, *Angew. Chem., Int. Ed. Engl.* **17**, 852 (1978).
2. M. B. Robin and P. Day, *Adv. Inorg. Chem. Radiochem.* **10**, 247 (1967).
3. J. A. Paradis, M.-H. Whangbo, and R. V. Kasowski, *New J. Chem.* **17**, 525 (1993).
4. K. Neininger, Thesis, Freiburg Univ., 1996.
5. M.-H. Whangbo and R. Hoffmann, *J. Am. Chem. Soc.* **100**, 6093 (1978).
6. A. Rabenau and H. Rau, *Inorg. Synth.* 160 (1973).
7. G. M. Sheldrick, "SHELXS86, Program for Crystal Structure Solution," Univ. of Göttingen, 1986.
8. G. M. Sheldrick, SHELXL93, Program for Crystal Structure Refinement, Univ. of Göttingen, 1993.
9. S. Parkin, B. Moezzi, and H. Hope, *J. Appl. Crystallogr.* **28**, 53 (1995).
10. P. Monceau, Ed., "Electronic Properties of Inorganic Quasi-One-Dimensional Compounds," Parts I and II. Reidel, Dordrecht, The Netherlands, 1985.
11. J. Rouxel, Ed., "Crystal Chemistry and Properties of Materials with Quasi-One-dimensional Structures." Reidel, Dordrecht, The Netherlands, 1986.
12. E. Canadell and M.-H. Whangbo, *Chem. Rev.* **91**, 965 (1991).
13. S. S. Dhingra, D.-K. Seo, G. W. Kowach, R. Kremer, J. Shreeve-Keyer, R. C. Haushalter, and M.-H. Whangbo, *Angew. Chem., Int. Ed. Engl.* **36**, 1087 (1997).